# OBLIQUE POLARIMETRIC SAR PROCESSOR BASED ON SIGNAL AND INTERFERENCE SUBSPACE MODELS

*F. Brigui*[*]*, L. Thiron-Lefevre*

Supélec, Sondra, France

*G. Ginolhac, P. Forster*

ENS Cachan, Satie UniverSud, France

## 1. INTRODUCTION

Detection of target in complex environment is a current issue in SAR community. For FoPen (Foliage Penetration) applications, many scatterers cause false alarms. To increase detection in such environment, SAR processors using the properties of the scattering of the target have been developed [1, 2]. Nevertheless, false alarms still remain as long as their scattering have common properties to that of the target. In this study, we propose a new SAR processor based on the oblique projection developed in [3] to reduce these false alarms . Instead of assuming that the clutter is only white Gaussian noise, we make the assumption that the clutter is made of structured noise too. This one is described by a physical model which defines the direction of the oblique projector. Considering this operator, we estimate the part of the scattering corresponding to the target only and we can process an image in which the target is detected and the interferences are reduced. Results on simulated data for FoPen application show the interest of this method.
The following convention is adopted : italic indicates a scalar quantity, lower case boldface indicates a vector quantity and upper case boldface a matrix. $T$ denotes the transpose operator and † the transpose conjugate.

## 2. PROBLEM STATEMENT

### 2.1. SAR Configuration and Notations

In SAR configuration, we consider that an antenna evolves along a linear trajectory ; at each position $u_i$, $i \in [\![1, N]\!]$ the antenna emits a signal and receives the response from the scene under observation. For more details on SAR configuration and process see [4]. The distance between adjacent positions is constant and equal to $\delta u$. The emitted signal is a chirp in polarization H ($p = H$) or V ($p = V$) with a frequency bandwidth $B$, a central frequency $f_0$ and a duration $T_e$. We denote by $\mathbf{z}_{pi} \in \mathbb{C}^K$ ($i \in [\![1, N]\!]$) the received signal samples at every $u_i$ position of the antenna either in horizontal polarization or in vertical polarization and $K$ is the number of time samples. The total received signal $\mathbf{z}_p$ for one polarization channel is the concatenation of the N vectors $\mathbf{z}_{pi}$ (see [1]) :

$$\mathbf{z}_p \in \mathbb{C}^{NK}, \quad \mathbf{z}_p = \begin{bmatrix} \mathbf{z}_{p1}^T & \mathbf{z}_{p2}^T & \dots & \mathbf{z}_{pN}^T \end{bmatrix}^T \tag{1}$$

The total polarimetric received signal $\mathbf{z}$ is then the concatenation of $\mathbf{z}_H$ and $\mathbf{z}_V$ : $\mathbf{z} \in \mathbb{C}^{2NK}, \quad \mathbf{z} = \begin{bmatrix} \mathbf{z}_H^T & \mathbf{z}_V^T \end{bmatrix}^T$
We precise that only the co-polarized channels are considered ($H = HH$ and $V = VV$).

### 2.2. Problem Modeling

We consider that man-made targets (MMT) are located at different pixels $t_i = (x_{t_i}, y_{t_i})$. To take into account the physical properties of the target scattering, we assume that a MMT can be modeled by a set of Perfectly Conducting (PC) plates having each one a different orientation described by the angles $(\alpha, \beta)$. The orientation $(\alpha, \beta)$ of the target is unknown. As this latter strongly influences the scattering pattern of this, we can not favor a single orientation. Thus our model has to take into account all the possible orientations of a target. We assume then that for any orientation $(\alpha, \beta)$ of the PC plate, our model belongs to a low-rank subspace, called $\langle H_{t_i} \rangle$ (for more details on this subspaces and its generation, see for one polarimetric channel [1] and

[*]Thanks to DGA (Direction Générale de l'Armement) for funding.

for co-polarized channels [2]). The modeling of $\mathbf{z}$ is written as :

$$\mathbf{z} = \sum_{t_i} \mathbf{H}_{t_i} \boldsymbol{\lambda}_{t_i} + \boldsymbol{\nu} \tag{2}$$

where $\mathbf{H}_{t_i}$ is an orthonormal basis of $\langle H_{t_i} \rangle$ and, $\boldsymbol{\lambda}_{t_i}$ is an unknown coordinate vector. $\nu$ is a vector of noise. This vector can be modeled in two ways :

– Unstructured Noise Case
We consider that the vector $\boldsymbol{\nu}$ is only a white Gaussian noise. Then the received signal may be rewritten as :

$$\mathbf{z} = \sum_{t_i} \mathbf{H}_{t_i} \boldsymbol{\lambda}_{t_i} + \mathbf{n} \tag{3}$$

where $\mathbf{n}$ is a Gaussian white noise of known variance $\sigma^2$. This is the more simple noise that we can consider and this modeling was used for SAR processor based on subspace detectors in [1, 2].

– Structured Noise Case
In complex environments such as for FoPen, several scatterers in addition of targets can have high responses. To take into account these responses, we consider that the noise vector $\boldsymbol{\nu}$ is made of two processes, structured noise and white Gaussian noise. For FoPen applications, the structured noise is due to the trees of the forest. Furthermore we restrain our study at P-band frequencies and thus we can consider that only trunks have a response. The trucks are then modeled by a dielectric cylinder lying on ground and whose orientation is described by the angles $(\gamma, \delta)$. As for the target, we suppose that the response of a trunk at a position $(x, y)$ belongs to a low-rank subspace $\langle J_{xy} \rangle$. At last, we do not make any assumption on the position of the trees as there are considered as noise. We denotes their positions by $c_i = (x_i, y_i)$. Then the noise vector $\nu$ and the received signal $\mathbf{z}$ are rewritten as follows :

$$\nu = \sum_{c_i} \mathbf{J}_{c_i} \boldsymbol{\mu}_{c_i} + \mathbf{n}$$

$$\mathbf{z} = \sum_{t_i} \mathbf{H}_{t_i} \boldsymbol{\lambda}_{t_i} + \sum_{c_i} \mathbf{J}_{c_i} \boldsymbol{\mu}_{c_i} + \mathbf{n} \tag{4}$$

where $\mathbf{J}_{c_i}$ is an orthonormal basis of $\langle J_{c_i} \rangle$ and $\boldsymbol{\mu}_{c_i}$ is an unknown coordinate vector.

## 3. SAR IMAGE PROCESSORS

### 3.1. Local Problem

The bases $\mathbf{H}_{t_i}$ and $\mathbf{J}_{c_i}$ depend on the pixels $t_i$ and $c_i$, and on the scattering pattern of our canonical models, the PC plate and the dielectric cylinder on ground. It have been shown in [1] that for a pixel $t_i$ and $c_i$, the bases can be written as :

$$\mathbf{H}_{t_i} = \boldsymbol{\Phi}_{t_i}^{Pol} \mathbf{H}_0 \qquad \mathbf{J}_{c_i} = \boldsymbol{\Phi}_{c_i}^{Pol} \mathbf{J}_0 \tag{5}$$

where $0 = (x_0, y_0)$ is a reference pixel. For any pixel $(x, y)$, the matrix $\boldsymbol{\Phi}_{xy}^{Pol}$ which contains the position dependency is defined as follows :

$$\boldsymbol{\Phi}_{xy}^{Pol} = \begin{bmatrix} \boldsymbol{\Phi}_{xy} & \mathbf{0} \\ \mathbf{0} & \boldsymbol{\Phi}_{xy} \end{bmatrix} \quad \text{with} \quad \boldsymbol{\Phi}_{xy} = \begin{bmatrix} \exp(-j2\pi f_0 \tau_1(x,y))\, \mathbf{I}_{\lceil T_e F_s \rceil} & & \mathbf{0} \\ & \ddots & \\ \mathbf{0} & & \exp(-j2\pi f_0 \tau_n(x,y))\, \mathbf{I}_{\lceil T_e F_s \rceil} \end{bmatrix} \tag{6}$$

where $F_s$ is the sample frequency and $\tau_i$ is the time delay between the radar at the position $u_i$ and the pixel $(x, y)$. This matrix is unitary, so $\boldsymbol{\Phi}_{xy}^{Pol\dagger} \boldsymbol{\Phi}_{xy}^{Pol} = \boldsymbol{\Phi}_{xy}^{Pol} \boldsymbol{\Phi}_{xy}^{Pol\dagger} = \mathbf{I}$. Initially, this matrix was introduced to reduce the computational cost of the generation of the bases in [1]. In this study, it allows us to express the global SAR received signal $\mathbf{z}$ as local received signal $\mathbf{z}_{xy} = \boldsymbol{\Phi}_{xy}^{Pol\dagger} \mathbf{z}$ from one pixel $(x, y)$ using the following hypothesis :

$$\begin{array}{rcll} \|\boldsymbol{\Phi}_{xy}^{Pol\dagger} \mathbf{H}_{t_i} \boldsymbol{\lambda}_{t_i}\|^2 & \approx & 0 & \text{if} \quad (x,y) \neq (x_{t_i}, y_{t_i}) \\ \|\boldsymbol{\Phi}_{xy}^{Pol\dagger} \mathbf{J}_{c_i} \boldsymbol{\mu}_{c_i}\|^2 & \approx & 0 & \text{if} \quad (x,y) \neq (x_{c_i}, y_{c_i}) \end{array} \tag{7}$$

This hypothesis means that we can distinguish the signal of two scatterers at different positions $(x_t, y_t)$ and $(x_c, y_c)$. This hypothesis is verified a posteriori in the SAR images in Section 4.
As we do not know the positions of the targets and the interferences, for one pixel $(x, y)$, we have :

– Unstructured noise case

$$\mathbf{z}_{xy} = \mathbf{H}_0 \boldsymbol{\lambda}_{xy} + \mathbf{n}_{xy} \tag{8}$$

– Structured noise case

$$\mathbf{z}_{xy} = \mathbf{H}_0 \boldsymbol{\lambda}_{xy} + \mathbf{J}_0 \boldsymbol{\mu}_{xy} + \mathbf{n}_{xy} \tag{9}$$

with $\mathbf{n}_{xy} = \Phi_{xy}^{Pol\dagger}\mathbf{n}$.

### 3.2. Estimation

For each pixel $(x, y)$, the estimation of $\boldsymbol{\lambda}_{xy}$ of the Eq.( 8) and Eq.( 9) is solved by mean of the linear least square [3] :

– Unstructured Noise Case

$$\hat{\boldsymbol{\lambda}}_{xy} = \mathbf{H}_0^{\dagger}\mathbf{z}_{xy} \tag{10}$$

– Structured Noise Case

$$\hat{\boldsymbol{\lambda}}_{xy} = \mathbf{H}_0^{\dagger}(\mathbf{I} - \mathbf{J}_0(\mathbf{J}_0^{\dagger}\mathbf{P}_{\mathbf{H}_0}^{\perp}\mathbf{J}_0)^{-1}\mathbf{J}_0^{\dagger}\mathbf{P}_{\mathbf{H}_0}^{\perp})\mathbf{z}_{xy} = \mathbf{H}_0^{\dagger}\mathbf{E}_{\mathbf{H}_0\mathbf{J}_0}\mathbf{z}_{xy} \tag{11}$$

where $\mathbf{E}_{\mathbf{H}_0\mathbf{J}_0}$ is the oblique projection whose range is $\langle H_0 \rangle$ and whose null space is $\langle J_0 \rangle$ [3].

### 3.3. Images

We define the intensities of the images as the square modulus of $\hat{\boldsymbol{\lambda}}_{xy}$ for each pixel $(x, y)$. Then we have for the processor in the unstructured noise case (SDSAR [1, 2]) :

$$I_{SDSAR}(x, y) = \|\hat{\boldsymbol{\lambda}}_{xy}\|^2 = \mathbf{z}_{xy}^{\dagger}\mathbf{P}_{\mathbf{H}_0}\mathbf{z}_{xy} \tag{12}$$

where $\mathbf{P}_{\mathbf{H}_0} = \mathbf{H}_0\mathbf{H}_0^{\dagger}$ is the orthogonal projector onto $\langle H_0 \rangle$. In the structured noise case (OBLISAR), the processor is expressed as follows :

$$I_{OBLISAR}(x, y) = \|\hat{\boldsymbol{\lambda}}_{xy}\|^2 = \mathbf{z}_{xy}^{\dagger}\mathbf{E}_{\mathbf{H}_0\mathbf{J}_0}\mathbf{z}_{xy} \tag{13}$$

We clearly see that with the SDSAR processor the received signal $\mathbf{z}$ is orthogonally projected onto $\langle H_0 \rangle$ ; however if we consider the case of the structured noise, the projection onto $\langle H_0 \rangle$ is parallel to the direction defined by $\langle J_0 \rangle$. In addition of canceling the white Gaussian noise and increasing the detection of the target, the OBLISAR permits us to generate an image in which the structured noise is also reduced.

## 4. RESULTS

We propose in this section to evaluate the performance of reduction of false alarm of the OBLISAR compared to the SDSAR. We apply these processors to FoPen simulated data.

### 4.1. Configuration

To simulate a MMT for FoPen applications, we simulate a metallic box on ground included in a simulated forest of trunks (see Fig. 1). The metallic box has a size of 2m x 1.5m x 1m and is located at the position $(110, -1, 0)$m ; his scattering is simulated with the commercial software FEKO [5] which takes into account all the scattering mechanisms (single and double bounce diffusion, edge effects). For the forest, only the trunks are simulated since they are the principal cause of the false alarms ; their scattering are simulated with COSMO [6]. We consider a flight between the first position $u_1 = -50m$ and the

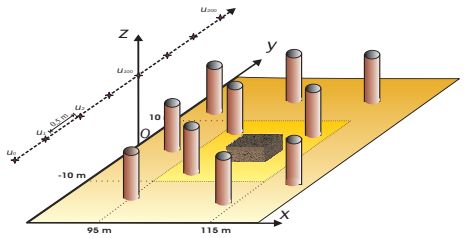


**Fig. 1**. SAR Configuration

last position $u_{200} = 50m$ with a $\delta_u = 0.5m$ between each position and an altitude of $100m$. The full polarized emitted signal is a chirp with a central frequency of $400MHz$, a bandwidth of $100MHz$ and of duration $2.10^{-7}s$. Finally, the radar scene is defined in $[90, 140]m$ for x-axis and $[-25, 20]m$ for y-axis.

### 4.2. Images

To generate the bases $\mathbf{H}_{xy}$ and $\mathbf{J}_{xy}$ for processing the SDSAR and the OBLISAR images, we choose a PC plate of size of $2mx1m$ and a dielectric cylinder of height of $11m$ and radius of $20cm$ for the model of the target and for the structured noise. The subspaces $\langle H_0 \rangle$ and $\langle J_0 \rangle$ have respectively a dimension of 6 and 10. In the Fig. 2(a), we present the SDSAR image ; the target is clearly detected but many false alarms due to the trees still remain. In the Fig. 2(b), we present the OBLISAR image. The target is still detected like. In addition, the false alarms are reduced. Thanks to the difference of physical properties of their scattering properties, the OBLISAR allows us to distinguish target from interferences and then to increase the response of the former while reducing the response of the latter.

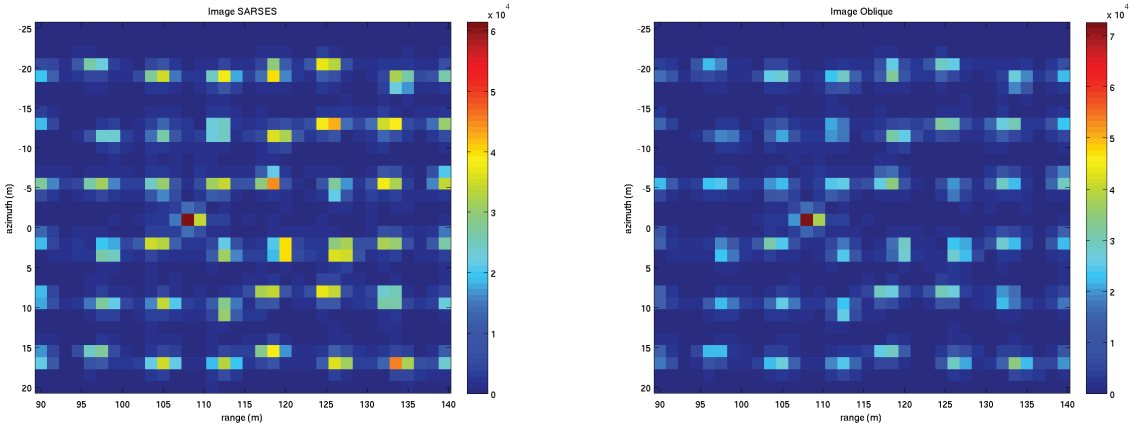


(a) (b)

**Fig. 2**. (a) SDSAR Image. (b) OBLISAR Image .

## 5. CONLUSION

We have presented in this study a new SAR processor, the OBLISAR, using the physical and polarimetric properties of the scattering of the target and the interferences. We have shown on simulated data the ability of the OBLISAR to detect target and to reduce false alarms in FoPen applications. For future work, we have to compute the performance of probability of detection and the probability of false alarms of the OBLISAR processor. Finally, we will apply this processor to real data.

## 6. REFERENCES


[1] R. Durand, G. Ginolhac, L. Thirion-Lefevre, and P. Forster, "New SAR processor based on matched subspace detector," *IEEE TAES*, vol. 45, no. 1, pp. 221 – 236, January 2009.

[2] F. Brigui, G. Ginolhac, P. Forster, and L. Thirion-Lefevre, "New polarimetric signal subpace detectors for SAR processors," in *ICASSP 2009 Tapei Taiwan*, April 2009.

[3] R.T. Behrens and L.L. Scharf, "Signal processing applications of oblique projection operators," *IEEE Trans. on Signal Processing*, vol. 42, no. 6, 1994.

[4] M. Soumekh, *Synthetic Aperture Radar Signal Processing*, Wiley - Interscience Publication, 1999.

[5] *Feko, User's Manual, EM Software and System*, 2004.

[6] L. Thirion, E. Colin, and C. Dahon, "Capabilities of a forest coherent scattering model applied to radiometry, interferometry and polarimetry at p and l bands," *IEEE TGRS*, vol. 44, no. 4, 2006.